Osteoporosis International (2019) 30:2271–2282
https://doi.org/10.1007/s00198-019-05117-0

ORIGINAL ARTICLE

Prediction of lumbar vertebral strength of elderly men based on quantitative computed tomography images using machine learning

M. Zhang[1] · H. Gong[1] · K. Zhang[1] · M. Zhang[2]

Received: 5 October 2018 / Accepted: 30 July 2019 / Published online: 10 August 2019

Abstract

Summary The parameters extracted from quantitative computed tomography (QCT) images were used to predict vertebral strength through machine learning models, and the highly accurate prediction indicated that it may be a promising approach to assess fracture risk in clinics.

Introduction Vertebral fracture is common in elderly populations. The main factor contributing to vertebral fracture is the reduced vertebral strength. This study aimed to predict vertebral strength based on clinical QCT images by using machine learning.

Methods Eighty subjects with QCT data of lumbar spine were randomly selected from the MrOS cohorts. L1 vertebral strengths were computed by QCT-based finite element analysis. A total of 58 features of each L1 vertebral body were extracted from QCT images, including grayscale distribution, grayscale values of 39 partitioned regions, BMD_{QCT}, structural rigidity, axial rigidity, and $BMD_{QCT}A_{min}$. Feature selection and dimensionality reduction were used to simplify the 58 features. General regression neural network and support vector regression models were developed to predict vertebral strength. Performance of prediction models was quantified by the mean squared error, the coefficient of determination, the mean bias, and the SD of bias.

Results The 58 parameters were simplified to five features (grayscale value of the 60% percentile, grayscale values of three specific partitioned regions, and $BMD_{QCT}A_{min}$) and nine principal components (PCs). High accuracy was achieved by using the five features or the nine PCs to predict vertebral strength.

Conclusions This study provided an effective approach to predict vertebral strength and showed that it may have great potential in clinical applications for noninvasive assessment of vertebral fracture risk.

Keywords Finite element analysis · Machine learning · QCT · Strength prediction · Vertebral body

Introduction

Osteoporosis (OP) is an age-related skeletal disorder that remarkably decreases bone mass and damages bone microstructure [1, 2]. Vertebral fracture is one of the major complications of OP. Among all osteoporotic fractures, vertebral compressive fracture (VCF) is very common in elderly populations. Symptomatic VCF can cause significant pain, portend future vertebral and hip fractures, and decrease patients' mobility with substantial impact on life quality [3]. It is difficult to diagnose and treat VCF in clinics. More than two thirds of VCF are not associated with injuries [4], and the incidence of subsequent fractures among treated patients is more than 20% [5]. The major causation of vertebral fracture is the reduced vertebral strength [1]; thus, accurate prediction of vertebral strength is the key to assessing and preventing the fracture risk.

With the development of computer technology and biomechanics, quantitative computed tomography-based finite element analysis (QCT/FEA) has been applied to assess bone strength in many clinical studies, in which the accurate information about geometry, architecture, and heterogeneous distribution of bone material properties are integrated in

✉ H. Gong
gonghe@jlu.edu.cn

[1] Department of Engineering Mechanics, Jilin University, Nanling Campus, Changchun 130025, People's Republic of China

[2] Department of Biomedical Engineering, The Hong Kong Polytechnic University, Hong Hum, Kowloon, Hong Kong SAR, People's Republic of China

accordance with the grayscale values in images [2]. Experimental results showed that QCT/FEA could effectively predict vertebral strength [6–9]. However, QCT/FEA modeling is difficult for widespread clinical use because of the complex modeling process and long computational time [10]. In order to avoid these problems, the parameter correlated with strength can be used to represent or estimate vertebral strength for assessing fracture risk.

There were numerous parameters related to bone strength that can be obtained from QCT images. The distribution of bone materials is a crucial material characteristic that may provide more precise information about bone "quality" compared with bone mineral density (BMD) [11]. Bone material properties are region-dependent [12]. The regional differences in BMD would lead to the regional variations in bone material properties, and bone material properties are related to its mechanical properties [13, 14]. Taken together, different regional distribution in BMD would ultimately lead to different mechanical properties [7]. Moreover, vertebral strength is also related to its geometry. Based on the engineering beam theory [15], the failure load of a whole bone is related to the area of the weakest cross-section and is proportional to the structural rigidity. Consequently, the middle cross-sectional area (A_{mid}) and the minimum cross-sectional area (A_{min}) of a vertebral body are considered the critical predictors of vertebral strength [16, 17]. In addition, a study indicated that the product of volumetric BMD (BMD_{QCT}) and A_{min} ($BMD_{QCT}A_{min}$) was significantly correlated with vertebral strength [2]. It was shown that the accuracy of bone strength prediction could be improved by combining some reasonable parameters as the predictors [18, 19]. Therefore, exploring the optimized parameter set based on QCT images to predict vertebral strength may have clinically potential in noninvasive assessment of fracture risk.

Recently, artificial intelligence, which developed rapidly in recent years, provides a new technical support for bone strength prediction. Machine learning belongs to a branch of artificial intelligence, which can automatically detect, learn, and master the relationships within data, then predict future data by applying the uncovered regulations [20]. Artificial neural network (ANN) and support vector regression (SVR) are the most frequently used machine learning algorithms for predicting bone strength [18, 19]. Using the second-order statistical features from the multi-detector CT images as input parameters, vertebral strength was accurately estimated by ANN model [21]. General regression neural network (GRNN), a type of ANN, needs only a fraction of the training samples and provides advantages to solve nonlinear regression problems [22]. In a recent study, SVR models were developed on the basis of the areal BMD (aBMD) and the geometric features of femoral head, and these trained models could predict proximal femoral strength effectively [19].

Accordingly, the aim of this study was to provide a direct approach to predict lumbar vertebral strength of elderly men by developing machine learning models based on the parameters from QCT images, including grayscale distribution, grayscale values of partitioned regions, BMD_{QCT}, structural rigidity, axial rigidity, and $BMD_{QCT}A_{min}$.

Materials and methods

Participants and QCT scanning procedures

Participants in this study were from the Osteoporotic Fractures in Men (MrOS) cohorts in Hong Kong part, in which 2000 elderly Chinese men were enrolled from the local communities between August 2001 and February 2003 [23]. All participants gave written informed consent [24]. To be eligible for the study, men needed to be aged at least 65 years, be able to walk without assistance from another person, and had not had bilateral hip replacement.

In this study, 80 subjects (aged 71.9 ± 4.2 years) with QCT data of lumbar spine were randomly selected from the participants to form the subcohort of the MrOS cohort. Differences in baseline characteristics of the subcohort and the entire MrOS cohort were compared using Student's *t* tests [24]. Age, weight, height, body mass index (BMI), and total hip aBMD for our study sample were similar to those for the full MrOS cohort (Table 1), confirming the validity of the random selection.

The QCT scans of lumbar spine (L1–L4) were taken using a standardized protocol. The settings of QCT scanning were 120 kVp, 205.95 mA, 1.25 mm slice thickness, 48 cm field of view, and 512 × 512 matrix in spiral reconstruction mode with 0.9375 mm/pixel size under a standard kernel (GE Medical Systems/LightSpeed 16, Wakesha, WI, USA). The QCT consecutive images were archived to Digital Imaging and communicated in DICOM format for further analysis [25]. The calibration phantom with three standard hydroxyapatite concentrations (0, 75, and 150 mg/cm^3), scanned with the participant, was included in the scan field (Image Analysis, Columbia, KY, USA) to convert CT grayscale value from Hounsfield units (HU) to equivalent BMD_{QCT} (g/cm^3) [8, 11].

Estimation of compressive strength of the L1 vertebral body

The QCT consecutive images of lumbar spine (L1–L4) for each subject were successively imported, rotated into a standard coordinate, thresholded, grown the region, and reconstructed to the three-dimensional model of L1 vertebral body (including cortical bone, cancellous bone, and vertebral endplates) in Mimics 17.0 software (Materialise, Leuven, Belgium) [7, 8]. Afterward, each QCT voxel was converted

Table 1 Mean (SD) baseline characteristics in the MrOS cohort compared with the randomly selected subcohort

	Full MrOS cohort	Subcohort	Significance level p
Age (years)	71.384 (4.342)	71.888 (4.213)	0.344
Weight (kg)	62.121 (8.932)	61.205 (8.225)	0.399
Height (cm)	162.866 (5.582)	163.027 (5.051)	0.812
BMI (kg/m^2)	23.409 (3.105)	23.023 (2.853)	0.306
Total hip aBMD (g/cm^2)	0.859 (0.123)	0.834 (0.109)	0.102

directly into a $1 \times 1 \times 1$ cm^3 voxel-type mesh of eight-node linear brick element (C3D8) [8]. To ensure that the upper and lower surfaces of vertebral body keep plano-parallel and to simulate loading conditions commonly used in the compression strength testing of cadaver vertebrae [15], two 1–3 mm layers of polymethylmethacrylate (PMMA) were virtually placed at the ends of each vertebral body model (Fig. 1a) [8]. After these procedures, the QCT/FEA models of L1 vertebral body were constructed. Then 150 kinds of material properties were assigned, and the QCT/FEA models were set to be heterogeneous transversely anisotropic. Besides, the values of yield/ultimate stress and corresponding plastic strains were computed to be used for the linearly elastic-linearly plastic nonlinear FEA. The proposed empirical relationships between elastic modulus (E_x, E_y, E_z), Poisson's ratio (ν_{xy}, ν_{xz}, ν_{yz}), shear modulus (G_{xy}, G_{xz}, G_{yz}), yield stress (σ_{ys}), and BMD_{QCT} for cancellous bone were as follows [13]:

$$E_z(MPa) = -34.7 + 3230 \times BMD_{QCT}\left(g/cm^3\right) \quad (1)$$

$$E_x = E_y = 0.333\,E_z \quad (2)$$

$$G_{xy} = 0.121\,E_z, \quad G_{xz} = G_{yz} = 0.157\,E_z \quad (3)$$

$$\nu_{xy} = 0.381, \quad \nu_{xz} = \nu_{yz} = 0.104 \quad (4)$$

$$\sigma_{ys}(MPa) = -0.75 + 24.9 \times BMD_{QCT}\left(g/cm^3\right) \quad (5)$$

The ultimate stress of each vertebral material in QCT/FEA models was considered 1.2 times its σ_{ys} [15], and the ultimate strain of all vertebral materials was set as 0.0145 [13]. The E_z and σ_{ys} were further multiplied by a constant factor of 1.28 to account for the side-artifact errors [7]. The material properties of PMMA were set to be isotropic ($E = 2500\,MPa, \quad \nu = 0.3$) [15].

After assignment of material properties, QCT/FEA models were imported into ABAQUS 6.14 software (Simulia, Providence, RI) to conduct standard/static analysis. As shown in Fig. 1 a, the uniform compressive displacement was applied to the nodes of upper surface of superior PMMA layer, and all the nodes on the lower surface of inferior PMMA layer were completely restrained [7, 9]. The compressive strength of each L1 vertebral body was computed as the total reaction force generated at an imposed overall deformation equivalent to 2% compressive strain [7, 9].

The parameters extracted from clinical QCT images

A total of 58 parameters of each vertebral body were extracted from the QCT images, including grayscale distribution, grayscale values of 39 partitioned regions, BMD_{QCT}, structural

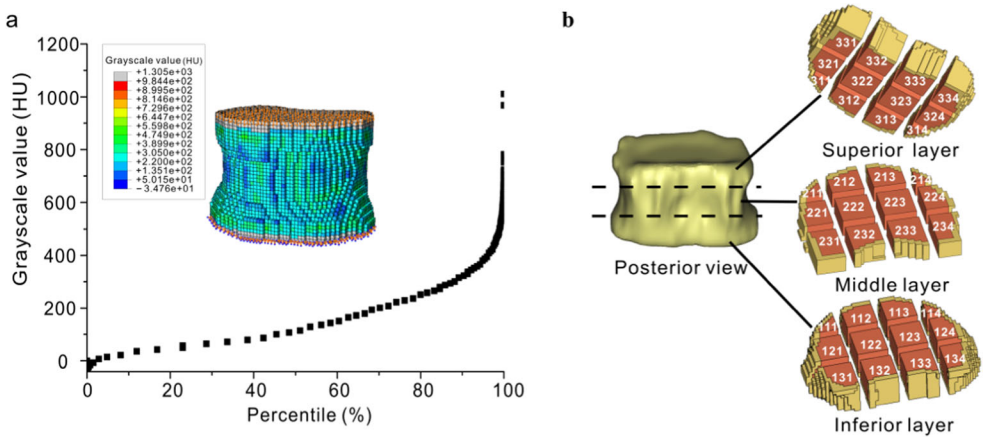

Fig. 1 The grayscale distribution within a typical L1 vertebral body model and the partition of cancellous bone. **a** The percentile plot of grayscale distribution with corresponding grayscale distribution of QCT/FEA model, in which the PMMA layers (gray color) are modeled and used for applying the boundary conditions. Compressive displacement is shown in orange color, and fixed displacement boundary condition is shown in blue and pink colors. **b** The schematic diagram of partition for cancellous bone of L1 vertebral body

rigidity, axial rigidity, and $BMD_{QCT}A_{min}$, as the predictors of vertebral strength and were numbered 1 to 58, respectively.

The grayscale distribution of L1 vertebral body

The material properties of QCT/FEA model were assigned in accordance with the grayscale values of bone voxels in QCT images. Therefore, in order to reflect the material distribution of vertebral body more clearly and directly, the grayscale distribution was used to represent the material distribution. The proportion of elements assigning to each grayscale value was calculated to obtain the frequency of each grayscale value for each vertebral body, and the percentile plot of the grayscale distribution for each vertebral body was drawn by transferring the frequency plot of the grayscale distribution (Fig. 1a). In this study, the grayscale distribution was described by the grayscale values with the percentiles of 1, 2, 5, 8, 10, 15, 20, 25, 30, 40, 45, 50, 60, 70, and 75%, which corresponded to the parameters with numbers 1 to 15, respectively.

Partition of L1 vertebral body and the grayscale values of the partitioned regions

To quantify the regional variations of grayscale values in vertebral body, 39 partitioned regions were set as follows: the region of whole vertebral body, the cortical bone region, the cancellous bone region, and the 36 subregions of cancellous bone. The grayscale value of each region was obtained by calculating the average grayscale value of the corresponding region. These grayscale values corresponded to the parameters with numbers 16 to 54, respectively.

The cancellous bone region was drawn alone in MIMICS 17.0, and the cortical bone region was obtained by Boolean operation between the regions of whole vertebral body and cancellous bone. A minimal cuboid covering cancellous bone was designed on the basis of the position coordinates of cancellous bone region, whose center was coincident with that of cancellous bone. The side lengths of the cuboid were equivalent to the maximum size of the vertebral body in each direction. The cuboid was divided into four parts in the left-right direction and three parts in both the anterior-posterior and superior-inferior directions, for a total of 36 parts. The segmented cuboid was used to partition cancellous bone of vertebral body into 36 corresponding regions, and the schematic diagram of partition and the numbers of regions are shown in Fig. 1 b. The partitioned region with the number of 111 was named as No. 111 region, the partitioned region with the number of 112 was named as No. 112 region, and so on.

BMD_{QCT}, structural rigidity, axial rigidity, and $BMD_{QCT}A_{min}$

In this study, four parameters that could indicate the vertebral strength were also considered as the features of vertebral body to improve the prediction accuracy: BMD_{QCT}, structural rigidity, axial rigidity, and $BMD_{QCT}A_{min}$, which corresponded to the parameters with numbers 55 to 58, respectively.

Using the calibration phantom with known hydroxyapatite mineral densities, the BMD_{QCT} of each L1 vertebral body was calculated as the mineral content contained in vertebral body divided by the corresponding volume. In addition to BMD_{QCT}, the QCT data were used to obtain other indices of bone strength using engineering beam theory [15]. Structural rigidity was calculated as the product of the average elastic modulus of vertebral body and its A_{mid}. Axial rigidity reflects the resistance of bone to tensile or compressive loading, and was calculated by the sum of the products between E_z of each bone voxel and its cross-sectional area. Moreover, $BMD_{QCT}A_{min}$ was equal to BMD_{QCT} times A_{min}.

Development of machine learning models for predicting vertebral strength

A total of 80 samples were randomly divided into the training set ($n = 58$) and the test set ($n = 22$). To avoid the curse of dimensionality and increase the prediction accuracy of machine learning models, the parameters extracted from QCT images were simplified by using feature selection and dimensionality reduction, respectively. Before the process of simplifying features, the correlations between QCT/FEA-computed vertebral strength and all parameters, namely, grayscale distribution, grayscale values of 39 partitioned regions, BMD_{QCT}, structural rigidity, axial rigidity, and $BMD_{QCT}A_{min}$, were investigated. The process of feature selection was as follows: from the 58 features, those highly correlated with QCT/FEA-computed strength were extracted and combined into different sets as input parameters of machine learning model. The parameter set with the best predictive results was selected as the optimized parameter set A, which could be used to predict vertebral strength. The process of dimensionality reduction was as follows: principal components analysis (PCA) was performed on the parameters that were significantly correlated with QCT/FEA-computed strength to identify the principal components (PCs) having the largest contribution to strength. Only PCs having eigenvalues greater than 1.0 were selected as input parameters for machine learning model [11]. These PCs were named as the optimized parameter set B, which could be used to predict vertebral strength.

In our study, two machine learning algorithms, GRNN and SVR, were designed to predict vertebral strength. To obtain the optimized prediction model and avoid over-fitting, the grid search method was adopted in which a range of parameter values were tested using the 10-fold cross validation strategy [26]. GRNN analysis and SVR analysis were programmed with MATLAB (MathWorks, Natick, USA) by using the Neural Network toolbox and the LIBSVM toolbox, respectively.

The procedure of predicting vertebral strength based on clinical QCT images is shown in Fig. 2. Prediction

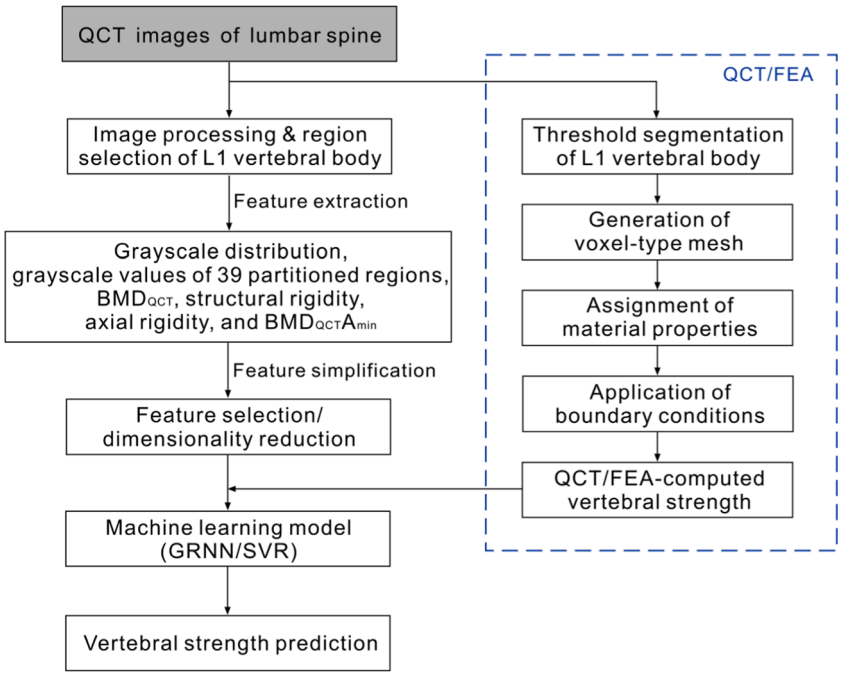

Fig. 2 The procedure of predicting vertebral strength based on clinical QCT images. The part with dotted line is the process of QCT/FEA, and the QCT/FEA-computed vertebral strengths were used to develop machine learning models

performance of machine learning models was quantified by the mean squared error (MSE), the coefficient of determination (R^2), the mean bias, and SD of bias, the last two performance indexes obtained from Bland-Altman analysis were used to evaluate the equivalence between QCT/FEA and machine learning models for vertebral strength.

Statistical analysis

In this study, the relationships between QCT/FEA-computed vertebral strength, grayscale distribution, grayscale values of 39 partitioned regions, BMD_{QCT}, structural rigidity, axial rigidity, and $BMD_{QCT}A_{min}$ were investigated using Pearson correlation. In addition, PCA was used for dimensionality reduction of 58 parameters to identify the PCs with large contribution to vertebral strength. Correlation analysis and PCA were performed by using SPSS 19.0 (BM Inc., Chicago, USA). The Bland-Altman analyses of QCT/FEA and machine learning derived vertebral strengths under the specific parameter sets were performed by using Prism software (GraphPad Software, San Diego, CA, USA). The significance level of p was set to be 0.05.

Results

Correlation analysis between QCT/FEA-computed strength and the extracted parameters

The QCT/FEA-computed vertebral strengths were 6385.03 ± 1485.17 N, ranging from 2974.96 to 9456.59 N. The correlation analysis indicated that the 58 parameters (i.e., grayscale distribution, grayscale values of 39 partitioned regions, BMD_{QCT}, structural rigidity, axial rigidity, and $BMD_{QCT}A_{min}$) were significantly correlated with QCT/FEA-computed vertebral strength ($p < 0.001$).

The performance of machine learning model for predicting vertebral strength

Simplifying the extracted parameters by feature selection

Due to the fact that the parameters were all significantly correlated with vertebral strength, 58 features can be selected to combine into different sets as input parameters of GRNN and SVR models. The prediction performances of machine learning models under different parameter sets were compared. Given the large number of parameter sets involved, only the prediction performances of specific machine learning models are listed (Table 2). As shown in Table 2, the MSE values of SVR models were less than those of GRNN models under the same parameter set, and the R^2 values of SVR models were higher than those of GRNN models. Among all the parameter sets, machine learning models achieved the best prediction performance by incorporating grayscale value of the 60% percentile, grayscale value of cortical bone, grayscale value of cancellous bone, and grayscale value of No. 221 region with $BMD_{QCT}A_{min}$. It was named optimized parameter set A. When the optimized parameter set A was used as input parameters of GRNN and SVR models, the MSE values were less than 0.011, the R^2 values were greater than 0.96, and the SD values of bias were less than 274.03 N (marked with italics in Table 2).

Table 2 The prediction performances of machine learning models under different input parameters

	Prediction model	Training set				Test set			
		MSE	R^2	Mean bias (N)	SD of bias (N)	MSE	R^2	Mean bias (N)	SD of bias (N)
Feature selection									
Numbers of parameter									
1–58	GRNN	0.012	0.94	35.20	348.47	0.047	0.87	− 155.40	400.57
	SVR	0.012	0.94	20.79	352.77	0.036	0.91	202.20	590.99
1–55	GRNN	0.041	0.80	80.93	629.07	0.117	0.72	469.78	855.20
	SVR	0.036	0.82	68.52	615.35	0.090	0.75	598.99	953.54
1–15	GRNN	0.045	0.73	− 53.40	654.33	0.096	0.66	422.24	1115.27
	SVR	0.040	0.75	− 33.53	689.75	0.012	0.69	443.23	1036.08
16–54	GRNN	0.039	0.82	− 10.50	535.40	0.088	0.68	− 349.47	969.14
	SVR	0.037	0.79	− 11.49	627.60	0.016	0.71	521.53	991.77
55–58	GRNN	0.011	0.94	6.87	336.45	0.015	0.94	− 39.10	451.10
	SVR	0.011	0.94	− 3.31	338.99	0.013	0.96	− 32.27	383.06
10–13, 16, 39, 56–58	GRNN	0.025	0.91	10.66	333.03	0.026	0.93	61.58	557.23
	SVR	0.011	0.94	− 14.55	346.59	0.016	0.96	126.67	395.76
13, 17, 18, 35, 56, 58	GRNN	0.017	0.94	1.79	283.99	0.016	0.95	90.14	482.24
	SVR	0.011	0.94	− 19.12	332.55	0.022	0.95	44.77	440.56
13, 16, 28, 39, 56	GRNN	0.010	0.94	14.63	290.54	0.016	0.95	60.42	461.66
	SVR	0.009	0.95	31.81	293.34	0.013	0.95	136.51	544.58
13, 17, 18, 35, 58	GRNN	*0.008*	*0.96*	*− 7.64*	*250.97*	*0.011*	*0.97*	*114.39*	*271.30*
	SVR	*0.007*	*0.96*	*− 2.10*	*274.03*	*0.010*	*0.97*	*− 85.53*	*270.69*
13, 18, 35, 58	GRNN	0.019	0.93	35.23	355.07	0.022	0.94	− 83.75	466.04
	SVR	0.012	0.94	− 2.10	343.05	0.015	0.96	97.20	400.14
Dimensionality reduction									
–	GRNN	0.009	0.97	47.99	241.51	0.009	0.96	7.17	268.40
	SVR	0.006	0.97	14.20	245.84	0.009	0.97	− 1.76	280.49

The best prediction performance of GRNN and SVR models in feature selection are marked in italics

Simplifying the extracted parameters by dimensionality reduction

The PCA revealed nine components that were above the 1.0-eigenvalue threshold, and these nine PCs (i.e., it was named optimized parameter set B) jointly explained 93.426% of data variation. Nine PCs were taken as input parameters of GRNN and SVR models, and the prediction performances of machine learning models are listed (Table 2). As shown in Table 2, the prediction performances of GRNN and SVR models were similar. The MSE values were less than 0.009, the R^2 values were greater than 0.96, and the SD values of bias were less than 280.49 N.

Bland-Altman plots of vertebral strengths derived from QCT/FEA and machine learning

Bland-Altman plots of QCT/FEA and machine learning derived strengths for the test set under the optimized parameter sets are shown in Fig. 3. Almost all data points were inside 95% confidence limits for the difference. It suggested that no trend between the differences in vertebral strengths derived from QCT/FEA and our trained machine learning models.

The validation of machine learning model

The well-trained machine learning models should be validated in terms of their ability to predict vertebral strength of new samples. Twenty elderly men with QCT data of lumbar spine were randomly selected from the local community hospitals in China, and the corresponding L1 vertebral bodies were used as validation samples. The ages of the subjects were 71.2 ± 4.2 years within the range of 65–79 years. The strengths of validation samples were predicted by machine learning models (GRNN and SVR models) under the specific input parameters (optimized parameter sets A and B), and then compared with the corresponding

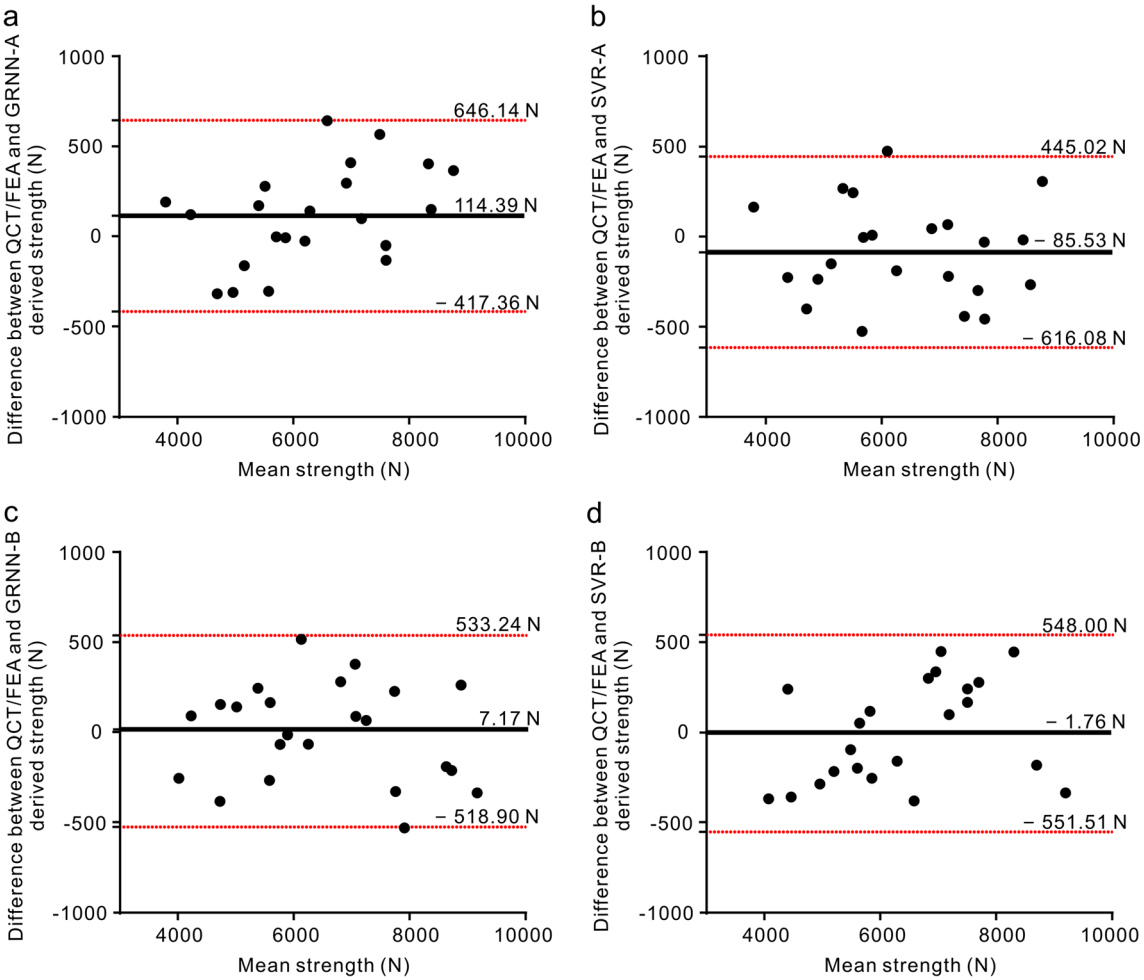

Fig. 3 Bland-Altman plots of QCT/FEA and machine learning derived strengths for the test set. **a** Bland-Altman plot of QCT/FEA and GRNN-A (GRNN model under optimized parameter set A) derived strengths. **b** Bland-Altman plot of QCT/FEA and SVR-A (SVR model under optimized parameter set A) derived strengths. **c** Bland-Altman plot of QCT/FEA and GRNN-B (GRNN model under optimized parameter set B) derived strengths. **d** Bland-Altman plot of QCT/FEA and SVR-B (SVR model under optimized parameter set B) derived strengths

QCT/FEA-computed strength. The absolute relative error (e) between them was computed as:

$$e = \frac{|S_{com} - S_{pre}|}{S_{com}} \times 100\% \quad (6)$$

where S_{com} is the strength computed from QCT/FEA model, and S_{pre} is the strength predicted from machine learning model.

The validation of machine learning model with the optimized parameter set A

The strengths of the 20 validation samples predicted by machine learning models with the optimized parameter set A were compared with the corresponding QCT/FEA-computed strengths, and the descriptive statistics of relative errors are shown in Table 3. For the 20 validation samples, the maximum relative errors between vertebral strengths obtained from QCT/FEA and machine learning models were 7.733 and 6.958%. All of the relative errors were less than 7.740%.

The validation of machine learning model with the optimized parameter set B

The strengths of the 20 validation samples predicted by machine learning models with the optimized parameter set B were compared with the corresponding QCT/FEA-computed strengths, and the descriptive statistics of relative errors are

Table 3 Descriptive statistics of relative errors between vertebral strengths obtained from QCT/FEA and machine learning models under the specific input parameters for the 20 validation samples

e (%)	Optimized parameter set A		Optimized parameter set B	
	GRNN	SVR	GRNN	SVR
Minimum	0.540	0.453	0.122	0.237
Maximum	7.733	6.958	7.443	6.908
Mean	4.192	4.117	4.006	3.828
SD	2.103	2.018	2.797	2.194

shown in Table 3. For the 20 validation samples, the maximum relative errors between vertebral strengths obtained from QCT/FEA and machine learning models were 7.443 and 6.908%. All of the relative errors were less than 7.450%.

Discussion

This study presents a direct approach to predicting compressive strength of lumbar vertebral body based on clinical QCT images by using machine learning, in which the material properties and geometric features of vertebral body were extracted from QCT images; GRNN and SVR were used as the machine learning algorithms to established prediction models. In this study, QCT/FEA-computed vertebral strengths were used as strength values to develop machine learning models, and the aim was to propose a more convenient and practical method for clinical strength prediction of vertebral body. Our results suggested that the approach achieved great prediction ability (Tables 2 and 3), and the vertebral strengths derived from QCT/FEA and our trained machine learning models have good consistency (Fig. 3). This promising approach has the advantages of simple modeling process and short computational time, and can be used by clinicians with a minimum training and no knowledge of FEA is required.

There are two reasons why we chose the L1 vertebral body in elderly men as subject. The first reason is that osteoporotic fractures in men are more prevalent than our general realization. Among persons older than 50 years of age, approximately 40% of all osteoporotic fractures worldwide occur in men [27], in which lumbar vertebral fracture is very common. Another reason is that lumbar vertebral fractures typically develop between L1 and L3 with the most frequently fractured site at L1 [28, 29], Thus, it is of great clinical significance to study L1 vertebral strength in elderly men.

Material properties and geometric features of vertebral body can be extracted from the QCT images. The material properties include integral material distribution and regional material distribution. In this study, integral material distribution was described by the grayscale values with the percentiles of 1, 2, 5, 8, 10, 15, 20, 25, 30, 40, 45, 50, 60, 70, and 75%. The reason why we used the grayscale values with specific 15 percentiles was to cover the range of cancellous bone distribution. These specific grayscale values mainly reflect cancellous bone "quality," and they were significantly correlated with vertebral strength. This result was in agreement with our previous study [11], in which the Young's moduli of cancellous bone materials with the percentiles of 0.5, 1, 2, 5, 8, 10, 15, and 20% were significantly correlated with femoral strength. In another study, the effects of PTH, Alendronate, and their combination on femoral strength were investigated, and it was found that these treatments positively affected femoral strength through their effects on density of cancellous bone [30]. These similar results suggested that cancellous bone "quality" makes great contribution to the maintenance of whole bone strength.

The integral material distribution parameters provide the information about cancellous bone "quality," and regional material distribution features can reflect the regional variations in bone material properties, both of them are essential for predicting vertebral strength. In this study, we used grayscale values of cortical bone, cancellous bone, and 36 subregions of cancellous bone to represent regional material distribution. The BMDs of cortical bone and cancellous bone are related to vertebral fracture risk. For young people, the majority of vertebral strength is maintained by cancellous bone [31]. However, cancellous bone has more active metabolic activities compared with cortical bone [32]. As a result, there is greater rate of bone loss in cancellous bone with age, and the relative contribution of cortical bone to vertebral strength tends to be greater in vertebrae with lower cancellous bone volume [31, 32]. On the other hand, each vertebral body has its specific proportion of cortical and cancellous bones, and the proportion may affect vertebral strength. Thus, it is crucial to obtain the grayscale values of cortical bone and cancellous bone for vertebral strength prediction.

Generally, vertebral fractures often occur in the region with low BMD [33], and BMD of cancellous bone is relatively lower in the vertebral body; thus, thoroughly understanding the regional variation in BMD of cancellous bone may help us to identify vertebral fracture site and fracture type. Grayscale value could be converted to equivalent BMD by the grayscale value–BMD relationship from QCT images and hence grayscale value could reflect BMD. Averaged over all 80 vertebral bodies, distributions of grayscale value within and among each of the three transverse layers of cancellous bone are shown in Fig. 4, and the white bolded number is the correlation coefficient between vertebral strength ($p = 0.000$) and grayscale value of each region. In the superior-inferior direction, there were significant differences in regional grayscale values between the three layers, and the regional grayscale values in the middle layer were significantly lower than those in the superior and inferior layers ($p < 0.005$). In the anterior-posterior direction, the average grayscale values of the 12 regions in the middle third of the centrum were 140.22 ± 31.42 HU, which was significantly lower than those of the 12 regions in both the anterior and posterior thirds of the centrum ($p = 0.001$). Coincidentally, there were relatively strong correlations between vertebral strength and grayscale values of Nos. 221 to 224 regions with correlation coefficients around 0.75. These results may explain why fracture sites tend to be located in the middle part of vertebral body under the uniaxial compression [1], and show the importance of considering BMD regional variations in the middle part (Nos. 221 to 224 regions) of vertebral body when predicting strength and assessing fracture risk.

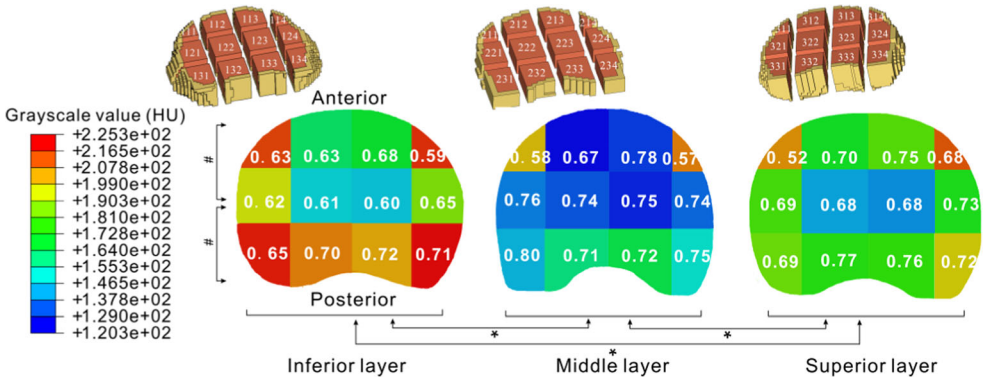

Fig. 4 Distributions of grayscale value within and among each region of cancellous bone in the three transverse layers. The color of each of the 36 regions corresponded to the average value over all 80 vertebral bodies, and the number labeled on each region was the correlation coefficient between vertebral strength ($p = 0.000$) and grayscale value of each region. * Significant difference between transverse layers ($p < 0.05$); # Significant difference between coronal layers ($p < 0.05$)

Cross-sectional area, such as A_{min} and A_{mid}, is the main geometric feature of vertebral body and is also a good predictor of vertebral compressive strength. In order to improve the prediction performance, we combined the relevant cross-sectional area with material properties or BMD_{QCT} as predictors since these combination parameters could predict vertebral strength with higher accuracy [15, 34–36]. As shown in Table 2, the machine learning models were relatively sensitive to the absence of structural rigidity, axial rigidity, and $BMD_{QCT}A_{min}$. For those machine learning models that did not use at least one of these three predictors as input parameters, their training performances (MSE ≥ 0.036, $R^2 \leq 0.82$, SD of bias ≥ 535.40) were much poorer compared with other prediction models (MSE ≤ 0.025, $R^2 \geq 0.91$, SD of bias ≤ 355.07). Moreover, structural rigidity, axial rigidity, and $BMD_{QCT}A_{min}$ were represented by the third principal component (PC3) in the PCA, which explained approximately 13.22% data variation. If nine PCs were used as input parameters except for PC3, the performances of machine learning models would degrade significantly (MSE ≥ 0.12, $R^2 \leq 0.48$, SD of bias ≥ 846.77). These results revealed that these three predictors make a great contribution to the prediction power of machine learning models.

Bone strength of patient cannot be directly predicted based on the features extracted from the QCT images, and it is usually assessed by means of specific algorithms. At present, there are many algorithms for solving prediction problems, which can be roughly divided into two categories: one is the traditional statistical method, such as linear regression; another is the machine learning algorithm, such as ANN and SVR [19, 37]. However, linear regression methods cannot accurately describe the relationship between independent and dependent variables in complex nonlinear problems. It was shown that the machine learning algorithms are clearly better equipped to appropriately process the input parameters and hence outperforms linear regression [19]. As shown in our study, the application of machine learning improved prediction performance and easily extends to computer-aided diagnosis applications in a clinical setting. The modular design of our approach, as detailed in Fig. 2, allows easy integration of different features or machine learning algorithms, which could facilitate further improvements in prediction performance and apply to clinical assessment efficiently. GRNN and SVR algorithms were used to predict vertebral strength in this study. To validate the well-trained GRNN and SVR models, the predicted strengths from 20 new subjects were compared with the corresponding QCT/FEA-computed strengths, and the relative errors between them were less than 7.750%. This validation suggested that these prediction models have good generalization ability and may capture the underlying susceptibility attributes of bone strength. However, our prediction models also require further validation for the prospective clinical prediction of vertebral strength.

In this study, the vertebral strengths for developing machine learning models were computed by QCT/FEA. The QCT data we used were from elderly men in the MrOS cohort and not from cadaver vertebrae, so we could not directly perform mechanical tests to obtain their vertebral strengths. FEA of QCT scans is the most technologically advanced method currently available for noninvasive clinical assessment of bone strength [38], and this technique has been well validated in cadaver studies [8, 15, 39, 40]. The finite element modeling method of vertebral body we used was consistent with that of previous studies [7, 9]. Results from cadaver biomechanical testing of vertebral bodies in men and women confirmed that this modeling method provided highly correlated estimates of vertebral compressive strength compared to the experimentally measured values ($R^2 > 0.85$) with statistical Y = X accuracy [8, 41]. For all the 80 subjects, the QCT/FEA-computed L1 vertebral strengths were 6385.03 ± 1485.17 N, ranging from 2974.96 to 9456.59 N, the values that are consistent with those measured in human lumbar vertebrae [6, 42, 43]. Moreover, the fracture sites of 80 vertebral bodies were defined as the point that reached the maximum plastic strain at the QCT/

FEA-computed vertebral strength [1], and 75% of them were located at the regions in the middle layer. These fracture sites have been shown to agree with the subsequent fracture locations [13, 44]. The above analyses showed that it is reasonable to use QCT/FEA to predict vertebral strength, and the comparisons with previous experiments in terms of strength and fracture site indirectly validated the accuracy of our QCT/FEA models. However, despite the above validation, it should be acknowledged that the QCT/FEA models still need to be fully validated by conducting cadaver biomechanical tests in future studies.

There are several limitations to our study. First, our QCT/FEA models did not include multiple loading conditions. The QCT/FEA-computed vertebral strengths were only based on single loading condition of axial compression. It was shown that the vertebral fracture risk may depend on applied load experienced during various activities [16], especially the load in forward bending [1]. However, previous studies indicated that the mechanical behaviors of the lumbar vertebra in axial compression and forward bending were strongly correlated [45]. Thus, we believed that the QCT/FEA-computed compressive strength of vertebral body could represent the strengths during other activities. Second, our GRNN and SVR models were based on the "black-box" approach that could not provide the mathematical expression between the inputs and outputs [20]. Nevertheless, machine learning algorithms could still predict vertebral strength for an individual patient and solve the regression problem that cannot be represented by specific expressions. Lastly, the well-trained machine learning models were derived from our own specific data sets (Chinese men aged over 65) and need to be validated by other cohort data. It is possible that the major contributing parameters of vertebral strength and their weight distributions may change in other populations (different sexes, ages, and ethnicities, etc.). Accordingly, we need to retrain machine learning models aiming at the new populations. Nevertheless, the current study provides a potential approach to estimate vertebral strength based on QCT images and suggestions for the selection of predictor variables that might improve bone strength assessment. Ultimately, this approach is hopeful to be used to increase the predictive ability of bone fracture risk in clinics.

In summary, the novelties of this study were that it obtained quantitative information that dominated the vertebral strength in elderly Chinese men, and provided a direct approach to estimate vertebral strength based on QCT images. Our results suggest that machine learning models can enhance computational efficiency with guaranteed precision and has great potential to be applicable for strength prediction of bones at other sites (such as femur and radius). The promising approach shows the great potential in clinical applications, and can non-invasively predict individual bone strength based on parameters of each patient. Therefore, this approach developed in this study may aid in improved assessment of subject-specific fracture risk and the development of individualized therapeutic intervention strategies.

Acknowledgments We wish to acknowledge the Osteoporotic Fractures in Men (MrOS) study. We are grateful to all of the participants in this study as well as all of the technicians who performed the scans.

Funding information This work is supported by the National Natural Science foundation of China (Nos. 11432016, 11872095, 11702110), the Natural Science foundation of Jilin Province (Nos. 20160101297JC, 20170519008JH, and 20170520093JH), and the Graduate Innovation Fund of Jilin University (No. 101832018C194).

Compliance with ethical standards

Conflicts of interest None.

References

1. Matsumoto T, Ohnishi I, Bessho M, Imai K, Ohashi S, Nakamura K (2009) Prediction of vertebral strength under loading conditions occurring in activities of daily living using a computed tomography-based nonlinear finite element method. Spine 34(14): 1464–1469. https://doi.org/10.1097/BRS.0b013e3181a55636
2. Dall'Ara E, Schmidt R, Pahra D, Varga P, Chevalier Y, Patsch J, Kainberger F, Zysset P (2010) A nonlinear finite element model validation study based on a novel experimental technique for inducing anterior wedge-shape fractures in human vertebral bodies in vitro. J Biomech 43(12):2374–2380. https://doi.org/10.1016/j.jbiomech.2010.04.023
3. Borgstrom F, Olafsson G, Strom O, Tillman JB, Wardlaw D, Boonen S, Miltenburger C (2013) The impact of different health dimensions on overall quality of life related to kyphoplasty and non-surgical management. Osteoporosis Int 24(7):1991–1999. https://doi.org/10.1007/s00198-012-2237-x
4. Song LJ, Wang LL, Ning L, Fan SW, Zhao X, Chen YL, Li ZZ, Hu ZA (2018) A modification and validation of quantitative morphometry classification system for osteoporotic vertebral compressive fractures in mainland Chinese. Osteoporosis Int 29(11):2495–2504. https://doi.org/10.1007/s00198-018-4641-3
5. Papanastassiou ID, Filis A, Gerochristou MA, Vrionis FD (2014) Controversial issues in kyphoplasty and vertebroplasty in osteoporotic vertebral fractures. Biomed Res Int 2014(934206):1–12. https://doi.org/10.1155/2014/934206
6. Lochmuller EM, Burklein D, Kuhn V, Glaser C, Muller R, Gluer CC, Eckstein F (2002) Mechanical strength of the thoracolumbar spine in the elderly: prediction from in situ dual-energy X-ray absorptiometry, quantitative computed tomography (QCT), upper and lower limb peripheral QCT, and quantitative ultrasound. Bone 31(1):77–84. https://doi.org/10.1016/S8756-3282(02)00792-5
7. Keaveny TM, Donley DW, Hoffmann PF, Mitlak BH, Glass EV, San Martin JA (2007) Effects of teriparatide and alendronate on vertebral strength as assessed by finite element modeling of QCT scans in women with osteoporosis. J Bone Miner Res 22(1):149–157. https://doi.org/10.1359/JBMR.061011
8. Wang X, Sanyal A, Cawthon PM, Palermo L, Jekir M, Christensen J, Ensrud KE, Cummings SR, Orwoll E, Black DM, Keaveny TM, Mros OFM (2012) Prediction of new clinical vertebral fractures in elderly men using finite element analysis of CT scans. J Bone Miner Res 27(4):808–816. https://doi.org/10.1002/jbmr.1539

9. Kopperdahl DL, Aspelund T, Hoffmann PF, Sigurdsson S, Siggeirsdottir K, Harris TB, Gudnason V, Keaveny TM (2014) Assessment of incident spine and hip fractures in women and men using finite element analysis of CT scans. J Bone Miner Res 29(3):570–580. https://doi.org/10.1002/jbmr.2069
10. Luo YH, Ahmed S, Leslie WD (2018) Automation of a DXA-based finite element tool for clinical assessment of hip fracture risk. Comput Meth Prog Bio 155:75–83. https://doi.org/10.1016/j.cmpb.2017.11.020
11. Gong H, Zhang M, Fan YB, Kwok WL, Leung PC (2012) Relationships between femoral strength evaluated by nonlinear finite element analysis and BMD, material distribution and geometric morphology. Ann Biomed Eng 40(7):1575–1585. https://doi.org/10.1007/s10439-012-0514-7
12. Yi C, Wang MY, Wei J, Wang J, Wang L, Cheng XG (2017) Preoperative QCT assessment of femoral head for assessment of femoral head bone loss. Exp Ther Med 13(4):1470–1474. https://doi.org/10.3892/etm.2017.4136
13. Mirzaei M, Zeinali A, Razmjoo A, Nazemi M (2009) On prediction of the strength levels and failure patterns of human vertebrae using quantitative computed tomography (QCT)-based finite element method. J Biomech 42(11):1584–1591. https://doi.org/10.1016/j.jbiomech.2009.04.042
14. Luo YH, Yang HJ (2019) Comparison of femur stiffness measured from DXA and QCT for assessment of hip fracture risk. J Bone Miner Metab 37(2):342–350. https://doi.org/10.1007/s00774-018-0926-z
15. Crawford RP, Cann CE, Keaveny TM (2003) Finite element models predict in vitro vertebral body compressive strength better than quantitative computed tomography. Bone 33(4):744–750. https://doi.org/10.1016/S8756-3282(03)00210-2
16. Bachmann KN, Bruno AG, Bredella MA, Schorr M, Lawson EA, Gill CM, Singhal V, Meenaghan E, Gerweck AV, Eddy KT, Ebrahimi S, Koman SL, Greenblatt JM, Keane RJ, Weigel T, Dechant E, Misra M, Klibanski A, Bouxsein ML, Miller KK (2016) Vertebral strength and estimated fracture risk across the BMI spectrum in women. J Bone Miner Res 31(2):281–288. https://doi.org/10.1002/jbmr.2697
17. Bruno AG, Broe KE, Zhang XC, Samelson EJ, Meng CA, Manoharan R, D'Agostino J, Cupples LA, Kiel DP, Bouxsein ML (2014) Vertebral size, bone density, and strength in men and women matched for age and areal spine BMD. J Bone Miner Res 29(3):562–569. https://doi.org/10.1002/jbmr.2067
18. Taylor M, Perilli E, Martelli S (2017) Development of a surrogate model based on patient weight, bone mass and geometry to predict femoral neck strains and fracture loads. J Biomech 55:121–127. https://doi.org/10.1016/j.jbiomech.2017.02.022
19. Yang CC, Nagarajan MB, Huber MB, Carballidogamio J, Bauer JS, Baum T, Eckstein F, Lochmüller E, Majumdar S, Link TM (2014) Improving bone strength prediction in human proximal femur specimens through geometrical characterization of trabecular bone microarchitecture and support vector regression. J Electron Imaging 23(1):013013. https://doi.org/10.1117/1.JEI.23.1.013013
20. Murphy KP (2012) Machine learning: a probabilistic perspective. MIT Press, Massachusetts
21. Nagarajan MB, Checefsky WA, Abidin AZ, Tsai H, Wang XX, Hobbs SK, Bauer JS, Baum T, Wismuller A (2015) Characterizing trabecular bone structure for assessing vertebral fracture risk on volumetric quantitative computed tomography. Proc SPIE Int Soc Opt Eng 9417(3):297–308. https://doi.org/10.1117/12.2082059
22. Panda BN, Bahubalendruni MVAR, Biswal BB (2015) A general regression neural network approach for the evaluation of compressive strength of FDM prototypes. Neural Comput Appl 26(5):1129–1136. https://doi.org/10.1007/s00521-014-1788-5
23. Harvey NC, Oden A, Orwoll E, Lapidus J, Kwok T, Karlsson MK, Rosengren BE, Ljunggren Ö, Cooper C, McCloskey E, Kanis JA, Ohlsson C, Mellström D, Johansson H (2018) Falls predict fractures independently of FRAX probability: a meta-analysis of the Osteoporotic Fractures in Men (MrOS) study. J Bone Miner Res 33(3):510–516. https://doi.org/10.1002/jbmr.3331
24. Orwoll ES, Marshall LM, Nielson CM, Cummings SR, Lapidus J, Cauley JA, Ensrud K, Lane N, Hoffmann PR, Kopperdahl DL, Keaveny TM, Osteoporotic Fractures in Men Study Group (2009) Finite element analysis of the proximal femur and hip fracture risk in older men. J Bone Miner Res 24(3):475–483. https://doi.org/10.1359/JBMR.081201
25. Yang L, Burton AC, Bradburn M, Nielson CM, Orwoll ES, Eastell R, Osteoporotic Fractures in Men (MrOS) Study Group (2012) Distribution of bone density in the proximal femur and its association with hip fracture risk in older men: the Osteoporotic Fractures in Men (MrOS) Study. J Bone Miner Res 27(11):2314–2324. https://doi.org/10.1002/jbmr.1693
26. Yoo TK, Kim SK, Kim DW, Choi JY, Lee WH, Oh E, Park EC (2013) Osteoporosis risk prediction for bone mineral density assessment of postmenopausal women using machine learning. Yonsei Med J 54(6):1321–1330. https://doi.org/10.3349/ymj.2013.54.6.1321
27. Johnell O, Kanis JA (2006) An estimate of the worldwide prevalence and disability associated with osteoporotic fractures. Osteoporosis Int 17(12):1726–1733. https://doi.org/10.1007/s00198-006-0172-4
28. Van Der Klift M, De Laet CEDH, McCloskey EV, Hofman A, Pols HAP (2002) The incidence of vertebral fractures in men and women: the Rotterdam Study. J Bone Miner Res 17(6):1051–1056. https://doi.org/10.1359/jbmr.2002.17.6.1051
29. Cooper C, Atkinson EJ, O'Fallon WM, Melton LJ (1992) Incidence of clinically diagnosed vertebral fractures: a population-based study in Rochester, Minnesota, 1985-1989. J Bone Miner Res 7(2):221–227. https://doi.org/10.1002/jbmr.5650070214
30. Keaveny TM, Hoffmann PF, Singh M, Palermo L, Bilezikian JP, Greenspan SL, Black DM (2008) Femoral bone strength and its relation to cortical and trabecular changes after treatment with PTH, alendronate, and their combination as assessed by finite element analysis of quantitative CT scans. J Bone Miner Res 23(12):1974–1982. https://doi.org/10.1359/jbmr.080805
31. Christiansen BA, Kopperdahl DL, Kiel DP, Keaveny TM, Bouxsein ML (2011) Mechanical contributions of the cortical and trabecular compartments contribute to differences in age-related changes in vertebral body strength in men and women assessed by QCT-based finite element analysis. J Bone Miner Res 26(5):974–983. https://doi.org/10.1002/jbmr.287
32. Chalhoub D, Orwoll ES, Cawthon PM, Ensrud KE, Boudreau R, Greenspan S, Newman AB, Zmuda J, Bauer D, Cummings S, Cauley JA, St OFMM (2016) Areal and volumetric bone mineral density and risk of multiple types of fracture in older men. Bone 92:100–106. https://doi.org/10.1016/j.bone.2016.08.014
33. Eswaran SK, Gupta A, Keaveny TM (2007) Locations of bone tissue at high risk of initial failure during compressive loading of the human vertebral body. Bone 41(4):733–739. https://doi.org/10.1016/j.bone.2007.05.017
34. Riggs BL, Melton LJ, Robb RA, Camp JJ, Atkinson EJ, Oberg AL, Rouleau PA, McCollough CH, Khosla S, Bouxsein ML (2006) Population-based analysis of the relationship of whole bone strength indices and fall-related loads to age- and sex-specific patterns of hip and wrist fractures. J Bone Miner Res 21(2):315–323. https://doi.org/10.1359/JBMR.051022
35. Buckley JM, Loo K, Motherway J (2007) Comparison of quantitative computed tomography-based measures in predicting vertebral compressive strength. Bone 40(3):767–774. https://doi.org/10.1016/j.bone.2006.10.025

36. Bouxsein ML, Melton LJ, Riggs BL, Muller J, Atkinson EJ, Oberg AL, Robb RA, Camp JJ, Rouleau PA, McCollough CH, Khosla S (2006) Age- and sex-specific differences in the factor of risk for vertebral fracture: a population-based study using QCT. J Bone Miner Res 21(9):1475–1482. https://doi.org/10.1359/JBMR.060606
37. Leslie WD, Lix LM (2014) Comparison between various fracture risk assessment tools. Osteoporosis Int 25(1):1–21. https://doi.org/10.1007/s00198-013-2409-3
38. Keaveny TM, Kopperdahl DL, Melton LJ, Hoffmann PF, Amin S, Riggs BL, Khosla S (2010) Age-dependence of femoral strength in white women and men. J Bone Miner Res 25(5):994–1001. https://doi.org/10.1359/jbmr.091033
39. Roberts BJ, Kopperdahl D, Thrall E, Muller JA, Keaveny TM, Bouxsein ML (2009) Prediction of femoral strength in a sideways fall configuration using QCT-based finite element analysis. Bone 44(S1):S72. https://doi.org/10.1016/j.bone.2009.01.158
40. Keyak JH (2001) Improved prediction of proximal femoral fracture load using nonlinear finite element models. Med Eng Phys 23(3):165–173. https://doi.org/10.1016/s1350-4533(01)00045-5
41. Crawford RP, Brouwers JEM, Keaveny TM (2004) Accurate prediction of vertebral strength using voxel-based non-linear finite element models. Trans Orthop Res Soc 29:1123
42. Moro M, Hecker AT, Bouxsein ML, Myers ER (1995) Failure load of thoracic vertebrae correlates with lumbar bone mineral density measured by DXA. Calcif Tissue Int 56(3):206–209. https://doi.org/10.1007/BF00298611
43. Dall'Ara E, Pahr D, Varga P, Kainberger F, Zysset P (2012) QCT-based finite element models predict human vertebral strength in vitro significantly better than simulated DEXA. Osteoporosis Int 23(2):563–572. https://doi.org/10.1007/s00198-011-1568-3
44. Imai K, Ohnishi I, Bessho M, Nakamura K (2006) Nonlinear finite element model predicts vertebral bone strength and fracture site. Spine 31(16):1789–1794. https://doi.org/10.1097/01.brs.0000225993.57349.df
45. Graeff C, Chevalier Y, Charlebois M, Varga P, Pahr D, Nickelsen TN, Morlock MM, Gluer CC, Zysset PK (2009) Improvements in vertebral body strength under teriparatide treatment assessed in vivo by finite element analysis: results from the EUROFORS study. J Bone Miner Res 24(10):1672–1680. https://doi.org/10.1359/JBMR.090416